Front. Biol. 2015, 10(3): 262–271
DOI 10.1007/s11515-015-1364-0

RESEARCH ARTICLE

Tbr2-expressing intermediate progenitor cells in the adult mouse hippocampus are unipotent neuronal precursors with limited amplification capacity under homeostasis

Daniel A. Berg[1,2,3,*], Ki-Jun Yoon[1,2,*], Brett Will[1], Alex Y. Xiao[1], Nam-Shik Kim[1,2], Kimberly M. Christian[1,2], Hongjun Song[1,2,4], Guo-li Ming (✉)[1,2,4]

[1] *Institute for Cell Engineering, Johns Hopkins University School of Medicine, Baltimore, MD 21205, USA*
[2] *Department of Neurology, Johns Hopkins University School of Medicine, Baltimore, MD 21205, USA*
[3] *Laboratory of Molecular Neurobiology, Department of Medical Biochemistry and Biophysics, Karolinska Institute, Scheeleväg 2, 17 117 Stockholm, Sweden*
[4] *The Solomon H. Snyder Department of Neuroscience, Johns Hopkins University School of Medicine, Baltimore, MD 21205, USA*

© Higher Education Press and Springer-Verlag Berlin Heidelberg 2015

Abstract **Neurogenesis persists in two locations of the adult mammalian brain, the subventricular zone of the lateral ventricles and the subgranular zone of the dentate gyrus in the hippocampus. In the adult subgranular zone, radial glial-like cells (RGLs) are multipotent stem cells that can give rise to both astrocytes and neurons. In the process of generating neurons, RGLs divide asymmetrically to give rise to one RGL and one intermediate progenitor cell (IPC). IPCs are considered to be a population of transit amplifying cells that proliferate and eventually give rise to mature granule neurons. The properties of individual IPCs at the clonal level are not well understood. Furthermore, it is not clear whether IPCs can generate astrocytes or revert back to RGLs, besides generating neurons. Here we developed a genetic marking strategy for clonal analysis and lineage-tracing of individual Tbr2-expressing IPCs in the adult hippocampus *in vivo* using *Tbr2-CreER^{T2}* mice. Using this technique we identified *Tbr2-CreER^{T2}* labeled IPCs as unipotent neuronal precursors that do not generate astrocytes or RGLs under homeostasis. Additionally, we showed that these labeled IPCs rapidly generate immature neurons in a synchronous manner and do not undergo a significant amount of amplification under homeostasis, in animals subjected to an enriched environment/running, or in animals with different age. In summary, our study suggests that Tbr2-expressing IPCs in the adult mouse hippocampus are unipotent precursors and rapidly give rise to immature neurons without major amplification.**

Keywords adult neurogenesis, Tbr2, clonal analysis, lineage tracing, enriched environment

Introduction

Neurogenesis is maintained in two distinct regions in the adult mammalian brain, the subventricular zone (SVZ) of the lateral ventricle and the subgranular zone (SGZ) of the dentate gyrus in the hippocampus (Ming and Song, 2011; Braun and Jessberger, 2013). In the adult mouse dentate gyrus, quiescent nestin^{+} radial glia-like cells (RGLs) as the resident multipotent stem cells can generate both neurons and astrocytes (Fig. 1A) (Bonaguidi et al., 2011). Prior to activation, RGLs start to express the proneuroal transcription factor Ascl1 and upon asymmetric neurogenic cell division, RGLs generate one RGL and one intermediate progenitor cell (IPC) (Kim et al., 2011; Lugert et al., 2012; Andersen et al., 2014). IPCs are thought to be a type of transit amplifying cells that undergo a series of symmetric divisions (Encinas et al., 2006). Early IPCs express high levels of Ascl1 and eventually start to express T-box brain protein 2 (Tbr2; also named Eomesodermin), a transcription factor known to be important in the transition from RGL to IPC (Englund et al., 2005; Hodge et al., 2008; Sessa et al., 2008). The IPCs later give rise to neuroblasts expressing doublecotin (DCX), which exhibit

Received May 22, 2015; accepted June 1, 2015
Correspondence: Guo-li Ming
E-mail: gming1@jhmi.edu

*These authors contributed equally to this work.

bipolar morphology with tangential processes (Fig. 1A) (Brown et al., 2003; Ming and Song, 2011). These neuroblasts differentiate into post-mitotic immature neurons, which develop dendrites projecting into the granule layer and a single axon into the hilus and gradually mature into functional and integrated granule neurons (van Praag et al., 2002; Ge et al., 2006; Faulkner et al., 2008;Toni et al., 2008; Sun et al., 2013).

Our knowledge of adult neurogenesis has increased dramatically in the last decade, yet the dynamic neurogenesis process *in vivo* is not fully understood. This is partially due to a lack of genetic tools to target specific precursor cell-types in a non-invasive manner with high temporal resolution. Previous studies have used transgenic mice, such as *Nestin-CreER*, *Glast-CreER* and *Hes5-CreER*, crossed with various reporter mice (Lugert et al., 2010; Bonaguidi et al., 2011; Encinas et al., 2011; DeCarolis et al., 2013), to investigate basic biology of adult neurogenesis. A caveat to these animal models is that recombination is not restricted to a specific precursor cell type in the dentate gyrus, making the study of the lineage relationships among different cell types difficult to assess. For example, the *Nestin-CreER* line labels RGLs, some IPCs and astroglia, while the *Hes5-CreER* line has been shown to label both RGLs and non-radial "horizontal stem cells," which have also been proposed to act as stem cells in the adult SGZ (Lugert et al., 2010; Bonaguidi et al., 2011). Additionally, most studies on adult neurogenesis focus on stem cells, while little is known of the lineage potential and clonal expansion capacity of IPCs. Individual neural stem cells in both adult SVZ and SGZ can generate a large number of neurons, and it is thought that IPCs act as transiently amplifying progenitor cells to generate multiple progeny from a single stem cell (Bonaguidi et al., 2011; Calzolari et al., 2015). For example, it has been calculated that IPCs in the adult SVZ divide 3 times, while each neuroblast divides 1–2 times (Ponti et al., 2013). The amplification stage in the adult SGZ is yet to be precisely determined. A recent fate-mapping study has suggested that the main amplification occurs in $DCX^+/Tbr2^+$ IPCs, based on the evidence that no significant amplification of the early $Ascl1^+$ DCX^- IPCs was observed (Lugert et al., 2012). On the other hand, analysis of cell cycle markers and BrdU pulse-chase experiments suggests that the DCX^- IPCs represent the majority of mitotically active neuronal precursors in the adult dentate gyrus (Kronenberg et al., 2003; Encinas et al., 2006). Quantitative analysis of individual IPCs is necessary to address their amplification capacity.

To study the development and clonal expansion of $Tbr2^+$ IPCs in a non-invasive manner, we generated a *Tbr2-CreER^{T2}* knock-in mouse line and crossed it with *mT/mG* or *ROSA-YFP* reporter mice. A single injection of tamoxifen resulted in recombination to label $Tbr2^+$ IPCs exclusively, with no other progenitor cells in the adult dentate gyrus were labeled. Unlike previous labeling methods used to study RGLs and IPCs in the adult SGZ, such as BrdU-based population studies, retroviral injections and *Nestin-CreER* mice, this *Tbr2-CreER^{T2}* mouse line enables us to study $Tbr2^+$ cells at the clonal level with no other progenitor cell-types labeled in the adult mouse SGZ. Using the *Tbr2-CreER^{T2}* mice, we examined the development and plasticity of $Tbr2^+$ IPCs with unprecedented temporal and cellular resolution *in vivo*.

Experimental procedures

Animals and tamoxifen injections

To generate the targeting vector for the *Tbr2-CreER^{T2}* allele, a 11.9 kb genomic fragment (from 5.8 kb upstream of exon 1 to 2.0 kb downstream of exon 5) was retrieved from C57BL/6J mouse genomic DNA BAC library (clone #RP24-77J5) and cloned into PL253 (pBSK vector containing thymidine-kinase (TK)) using recombineering (Liu et al., 2003). *CreER^{T2}-pA-frt-Neo-frt* cassette (modified from Addgene plasmid #14797) was inserted at the translation start site by recombineering, resulting in 5′ homology region (6.3 kb) and 3′ homology region (1.4 kb). Linearized targeting vector was electroporated into 129 SvEv ES cells, and neomycin and FIAU resistant ES cell colonies were screened by PCR. Two independent correctly targeted ES cell clones were used to generate germline chimeras. F1 progeny and subsequent generations were genotyped by PCR using following general Cre primers: 5′-TGC CAC GAC CAA GTG ACA GCA ATG-3′ and 5′-ACC AGA GAC GGA AAT CCA TGG CTC-3′ with the amplicon of 400 bp. The mouse line was maintained after backcrossing six times to C57BL/6 strain. The following reporter mice were purchased from Jackson Laboratories: *Rosa-YFP$^{f/f}$* (Strain: B6.129X1-Gt (ROSA)$^{26Sortm1(EYFP)Cos}$/J; Stock: 006148), *mT/mG$^{f/f}$* (Strain: B6.129(Cg)-*Gt(ROSA)26Sor$^{tm4(ACTB-tdTomato,-EGFP)Luo}$*/J; Stock: 007676). *Tbr2-CreER$^{T2/+}$* ::*mT/mG $^{f/+}$* and *Tbr2-CreER$^{T2/+}$* :: *Rosa-YFP* were generated by breeding *Tbr2-CreER$^{T2/+}$* with *mT/mG$^{f/f}$* or *YFP$^{f/f}$*. Recombination was induced in *Tbr2-CreER$^{T2/+}$*::*mT/mG$^{f/+}$* or *Tbr2-CreER$^{T2/+}$* ::*YFP$^{f/+}$* animals by a single injection of 186 mg/kg tamoxifen (62 mg/mL; Sigma; T5648), made with a 5:1 ratio of corn oil:ethanol and injected i.p. to 2 month-old mice. Six month-old mice were given an injection of 217 mg/kg tamoxifen. For enrichment treatment, mice had access to running wheels and numerous poly-carbonate tubes of different sizes and shapes.

All institutional and national guidelines for the care and use of laboratory animals were followed. Animals were housed in a 14 h light/10 h dark cycle with unlimited access to food.

Immunohistochemistry and confocal imaging and processing

Mice were anesthetized and transcardially infused with saline and then 4% paraformaldehyde. Brain sections were sectioned coronally (45 μm thickness) and maintained in

serial order throughout the entire dentate gyrus. Immunohistology was performed using following antibodies as previously described (Ge et al., 2006; Bonaguidi et al., 2011; Kim et al., 2012): anti-DCX (Santa Cruz; Goat; 1:500), anti-GFP (Rockland; Goat; 1:1000), anti-GFP (Aves; Chicken; 1:500), anti-MCM2 (BD (BM28); 1:500) and anti-Tbr2 (Abcam; Rabbit 1:500). For MCM2 staining, antigen retrieval was performed using DAKO retrieval solution (Dako S1699) at 95°C for 20 min and then 20°C for 10 min. GFP^+ cells were identified with an Axiovert 200M microscope (Zeiss) and then acquired as z-stacks on Zeiss 710 single-photon confocal microscope using 40X or 63X objectives. Clones spanning multiple sections were serially aligned using Reconstruct 1.1.0 (John C. Fiala, Human Brain Project, the National Institutes of Health) as previously described (Bonaguidi et al., 2011). Full resolution aligned images were exported into Imaris 7.1.1 (Bitplane) with voxel sizes adjusted according to dimensions specified in the LSM file for visualization of reconstructed clone in 3D.

Clonal analysis

Analyzed areas included the molecular layer, granule cell layer, SGZ and the hilus of the dentate gyrus. Sections were first screened for GFP^+ cells. Multiple cells were considered to be part of the same clone if the distance between the cells was less than 100 μm, based on previous computational simulation (Bonaguidi et al., 2011). Cell types were defined by morphological and immunohistological criteria as previously described (Bonaguidi et al., 2011). IPCs were defined by their small compact soma in the SGZ and multiple processes, neuroblasts were located in the SGZ and are bipolar with tangential processes, immature neurons were situated in the SGZ or apical granule cell layer with a thin dendrite extending through the granule cell layer. GFP^+ cells were counted as positive when $DAPI^+$ nuclei were completely encompassed by GFP in the case of mT/mG reporter or filled with GFP in case of YFP reporter. We observed consistent results using both mT/mG and YFP reporter (data not shown).

Results

A genetic strategy for specific targeting individual Tbr2-expressing IPCs in the adult mouse dentate gyrus

Previous studies using *in vivo* clonal analysis in adult SGZ have shown that individual nestin-expressing RGLs are multipotent neural stem cells, capable of both self-renewal and generating astrocytes and IPCs that eventually differentiate into neurons (Bonaguidi et al., 2011; Song et al., 2012; Jang et al., 2013). Since each labeled RGL can generate multiple IPCs over time, it is not possible to study the development of individual IPCs with high temporal resolution using this technique. To label IPCs specifically, we developed a tamoxifen-inducible Cre-transgenic, *Tbr2-CreER^{T2}* knock-in line, which expresses $CreER^{T2}$ under the endogenous control of the Tbr2 locus (Fig. 1B; See Experimental Procedures). The *Tbr2-CreER^{T2}* mice were then crossed with either *mT/mG* (Muzumdar et al., 2007) or *Rosa-YFP* (Srinivas et al., 2001) reporter mice (Fig. 1B). A single injection of tamoxifen (217 mg/ kg bodyweight; i.p. injection; 2-month-old animals), resulted in ~10 GFP^+ clones in the SGZ of each dentate gyrus (Fig. 1C), which remained constant when examined at multiple time points after injection (Fig. 1G). At 1 day post injection (dpi), 100% of GFP^+ cells in expressed both Tbr2 and doublecortin (DCX; n = 3 dentate gyri; Figs. 1D–1F). Importantly, no RGLs or astrocytes were labeled at 1 dpi (n = 8 dentate gyri). Taken together these results demonstrated that the *Tbr2-CreER^{T2}* line is a useful tool to study lineage potential, clonal expansion and differentiation of individual $Tbr2^+$ IPCs in adult hippocampus *in vivo*.

Lineage potential and differentiation of Tbr2-expressing IPCs in the adult dentate gyrus

IPCs are known to differentiate into neurons, but the exact tempo of IPC development has not been examined at the clonal level. It has also not yet been determined whether IPCs only generate neurons or if they have the potential to generate astrocytes or revert back to RGLs in the adult dentate gyrus under physiological conditions. To determine the fate of $Tbr2^+$ IPCs, we analyzed different time points upon tamoxifen induction and examined cell identity using both immunohistological and morphological criteria (Bonaguidi et al., 2011). Expression of Tbr2 was maintained in a majority of GFP^+ cells at 1 and 2 dpi, but only in 14%±4% of them at 4 dpi (n = 3 dentate gyri; Figs. 2A–B), indicating that $Tbr2^+$ IPCs rapidly develop into $Tbr2^-$ progenitor cells. To further evaluate differentiation of $Tbr2^+$ IPCs, we analyzed the morphology of GFP^+ cells at different time points (Figs. 2C and 2D). At 1 dpi, 90 %±4% of GFP^+ cells exhibited clear features of early IPCs (Figs. 2A and 2B), such as small compact soma with multiple processes (n = 8 dentate gyri). At 4 dpi, 72%±4% of GFP^+ cells showed features of NBs with bipolar morphology and long tangential processes. At 6 dpi, 79%±8% had turned into immature neurons with apical dendrites extending through the granular layer and a single short axon into the hilus (n = 6 dentate gyri). At 15 dpi, 100% of GFP^+ cells extended dendrites through the granule layer and the dendritic arborization became more elaborate (n = 8 dentate gyri). Importantly, we did not observe any GFP^+ astrocytes or RGLs at any time points after tamoxifen injection. Taken together, these results showed that $Tbr2^+$ IPCs rapidly and, in a rather synchronous manner, differentiate into immature neurons under homeostasis. Further, IPCs genetically labeled with our approach are unipotent

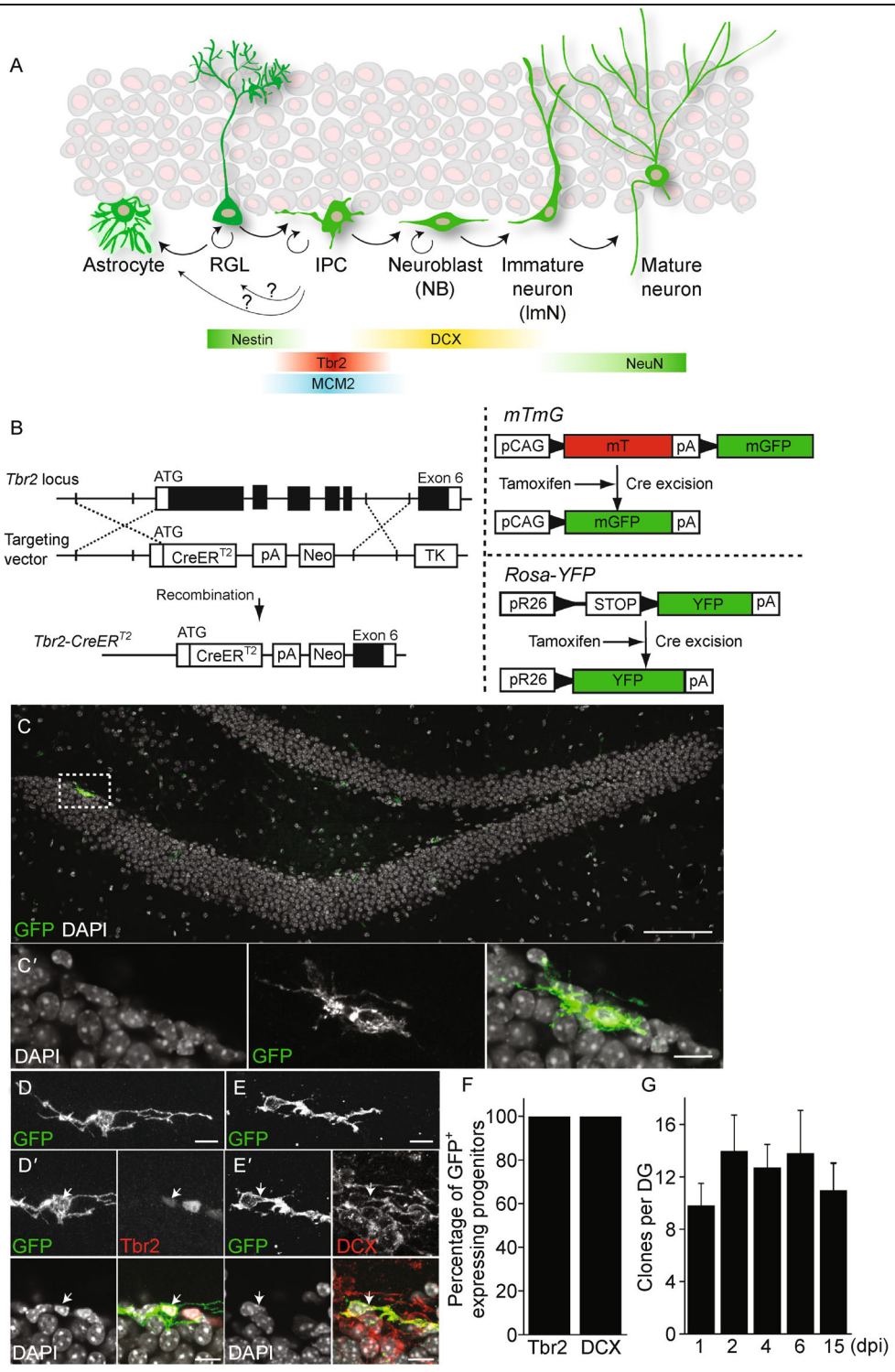

Figure 1 *Tbr2-CreER^{T2}* mouse line as a genetic tool to specifically target individual Tbr2^{+} IPCs in the adult mouse dentate gyrus. (A) A schematic diagram illustrating the lineage relationships during adult neurogenesis in the mouse hippocampus and the expression of markers used in this study. (B) An illustration of the genetic approach used to label individual Tbr2^{+} IPCs. (C–G) Lineage tracing of Tbr2-expressing IPCs at the clonal level. Adult mice were given a single injection of tamoxifen and examined at different time points. Shown in C is a sample confocal image of GFP^{+} precursors and DAPI in the adult dentate gyrus at 1 dpi (Scale bar: 100 μm). Magnification of boxed area in C is shown in C′ (Scale bar: 10 μm). Shown in D is a sample confocal image of a Tbr2^{+}GFP^{+} precursor at 1 dpi (Scale bar: 10 μm). Images of Tbr2 immunostaining and DAPI are shown in D′. Arrows point to GFP^{+} cells. Shown in E is a sample confocal image of a DCX^{+}GFP^{+} precursor at 1 dpi (Scale bar: 10 μm). Images of DCX immunostaining and DAPI are shown in D′. Shown in F are percentages of GFP^{+} progenitor cells expressing Tbr2 and DCX at 1 dpi. Values represent mean±SEM (n = 3 dentate gyri). Shown in G is a summary of quantification of the number of GFP^{+} clones per dentate gyrus at different time points. Values represent mean±SEM (n = 5–8 dentate gyri).

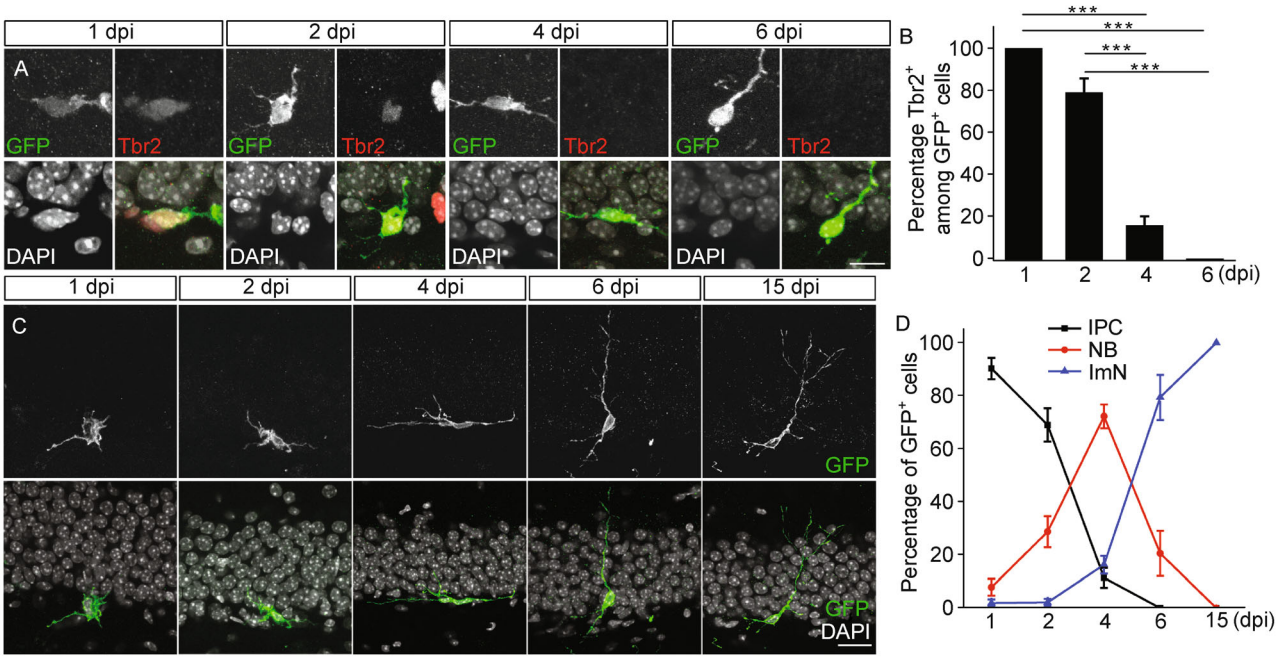

Figure 2 Clonally labeled Tbr2$^+$ IPCs rapidly change morphology and differentiate into immature neurons in the adult mouse dentate gyrus. (A–B) Time course of Tbr2 expression in GFP$^+$ cells in the dentate gyrus of adult *Tbr2-CreER^{T2}* mice upon a single injection of tamoxifen. Shown in A are sample confocal images of GFP, Tbr2 immunostaining and DAPI. Scale bar: 10 µm. Shown in B is a summary of percentages of GFP$^+$ cells expressing Tbr2 at different time points. Values represent mean±SEM (n = 3–4 dentate gyri; ***$p < 0.001$; One way ANOVA, Tukey's multiple comparisons test). (C–D) Development of GFP$^+$ cells in the dentate gyrus of adult *Tbr2-CreER^{T2}* mice upon a single injection of tamoxifen. Shown in C are sample confocal images of GFP and DAPI. Scale bar: 20 µm. Shown in D is a summary of quantitative comparison of different cell types at different time points. Values represent mean±SEM (n = 6–8 dentate gyri).

neural precursors that do not generate any RGLs or astrocytes under physiological conditions.

Clonal expansion and proliferative capacity of Tbr2-expressing IPCs

To determine the clonal expansion of individual Tbr2$^+$ progenitor cells over time, we quantified the number of GFP$^+$ cells in each clone at different time points upon tamoxifen injection (Figs. 3A and 3B). The largest clones were found at 1 and 2 dpi (2.2±0.1 and 2.3±0.1 cells per clone respectively), while at 15 dpi there was an average of 1.2±0.1 cells per clone (Fig. 3C). These data showed that there is no substantial expansion of the clone size of IPCs labeled using our approach. Rather, the clone size was significantly reduced at 4, 6 and 15 dpi compared to both 1 and 2 dpi, respectively ($p < 0.001$; One way ANOVA, Tukey's multiple comparisons test).

To examine to what extent *Tbr2$^+$-CreER^{T2}* traced cells remained in active cell cycle, we examined the expression of the cell cycle marker MCM2 at 1, 4, 6 and 15 dpi (Figs. 3D and 3E). We found that 100% of GFP$^+$ cells expressed MCM2 at 1 dpi, 90%±6% at 4 dpi, 13%±0.6% at 6 dpi, and 0% at 15 dpi (n = 3 dentate gyri, 19–34 GFP$^+$ cells per time point).

Taken together, these data showed that *Tbr2-CreER^{T2}* labeled IPCs do not undergo significant amplification and on average generate 1.2 immature neurons after 15 days.

Effect of enriched environment and voluntary exercise on Tbr2-expressing IPCs in the adult dentate gyrus

A paradigm of enriched environment and voluntary running is known to increase adult hippocampal neurogenesis and the number of Tbr2$^+$ cells in the adult dentate gyrus (Kempermann et al., 1997; van Praag et al., 1999; Hodge et al., 2008). Interestingly, the increase in proliferation can be observed after only 24 h of running (Steiner et al., 2008). Since most previous studies were performed at the population level, it is difficult to decipher whether the increase in the number of IPCs is solely due to increased activation of RGLs, or a combination of RGL activation and increased proliferation and survival of IPCs.

To determine the effect of an enriched environment and voluntary running treatment (EE) on individual IPCs, we injected a clonal dose of tamoxifen and placed mice in cages containing running wheels and polycarbonate tubes of different sizes and shapes for 4 days, while control mice were housed in normal cages (Fig. 4A). We found that subjecting animals to EE did not change the size of the *Tbr2-CreER^{T2}* labeled clones (Figs. 4B and 4D). Instead, there was a decrease in the number of GFP$^+$ precursors that expressed

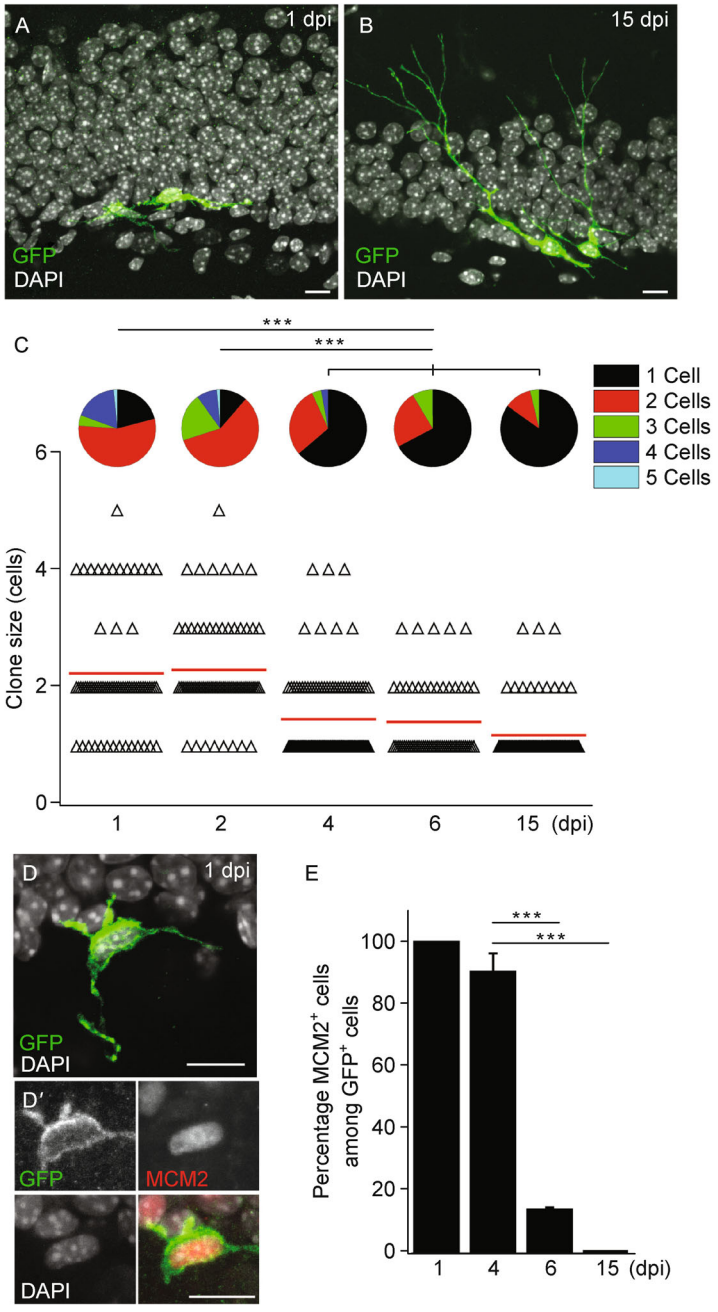

Figure 3 Proliferative capacity of Tbr2$^+$ IPCs in the adult mouse dentate gyrus. (A–B) Sample confocal image of GFP$^+$ clones containing multiple cells at 1 dpi (A) and 15 dpi (B). Scale bars: 10 µm. (C) Distribution of the clone size at different time points after a single tamoxifen injection. Pie charts indicate percentages of clones of different size and bars indicates mean (1 dpi: $n = 67$; 2 dpi: $n = 70$; 4 dpi: $n = 102$; 6 dpi: $n = 58$; 15 dpi: $n = 79$ clones, 5–8 dentate gyri per time point; ***$p < 0.001$; One way ANOVA, Tukey's multiple comparisons test). (D) A sample confocal image of an MCM2$^+$ GFP$^+$ cell at 1 dpi. Shown in D′ are images of GFP, MCM2 immunostaining and DAPI. Scale bar: 10 µm. (E) Summary of percentages of MCM2$^+$ GFP$^+$ cells at different time points after a single tamoxifen injection. Values represent mean±SEM ($n = 3$ dentate gyri; ***$p < 0.001$; One way ANOVA, Turkeys multiple comparisons test).

the cell cycle marker MCM2, suggesting that EE leads to accelerated cell cycle exit of Tbr2$^+$ IPCs (Figs. 4B, 4C and 4E). To examine the impact of on differentiation, we quantified different cell types in each clone. We found that animals subjected to EE exhibited fewer neuroblasts and increased immature neurons among GFP$^+$ cells when compared to control animals ($n = 6$–8 dentate gyri; Fig. 4F).

Taken together these data showed that the paradigm of enriched environment and running does not increase the survival or self-renewal of the *Tbr2-CreER^{T2}* traced-IPCs, but

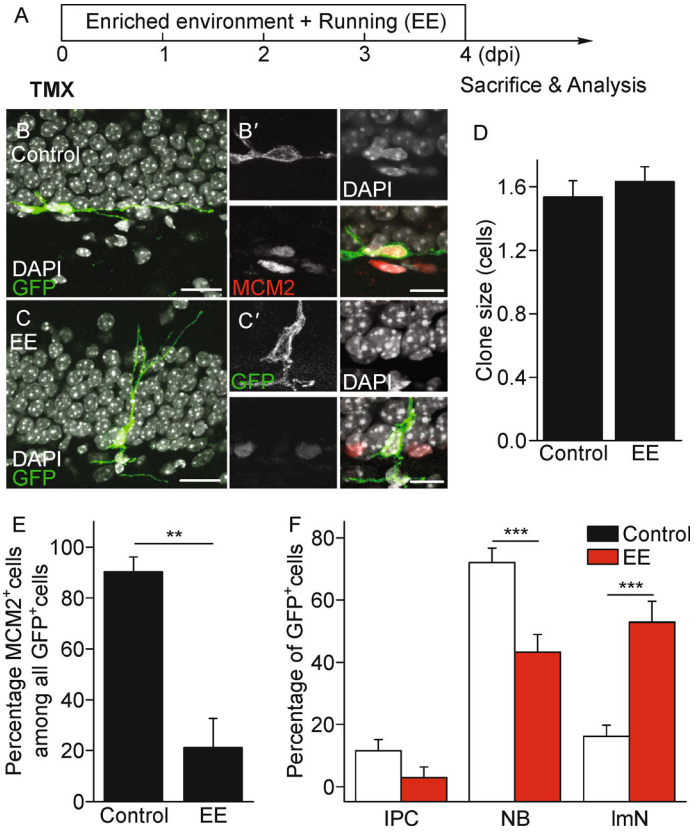

Figure 4 Paradigm of enriched environment and running accelerates the differentiation of Tbr2$^+$ IPCs in the adult mouse dentate gyrus. (A) A schematic illustration of the experimental paradigm used. (B–C) Sample confocal images of MCM2$^+$ GFP$^+$ cells in control animals (B) or animal subjected to enriched environment (EE, C) at 4 dpi. Scale bars: 20 μm. Shown in B′ and C′ are sample confocal images of GFP, MCM2 immunostaining and DAPI. Scale bars: 10 μm. (D) Summary of quantitative comparison of the clonal size at 4 dpi. Values represent mean±SEM (n = 6–8 dentate gyri). (E) Summary of quantitative comparison of percentages of MCM2$^+$ cells among all GFP$^+$ precursors. Values represent mean±SEM (n = 3 dentate gyri; *$p < 0.05$; **$p < 0.01$; Students t-test). (F) Summary of quantitative comparison of percentages of cell types observed in GFP$^+$ clones at 4 dpi. Values represent mean±SEM (n = 6–8 dentate gyri; ***$p < 0.005$; Student's t-test).

instead promotes cell cycle exit and accelerates their differentiation into immature neurons.

Tbr2-CreER^{T2} lineage-tracing in 6 month-old animals

The rate of adult neurogenesis is strongly reduced with age (Kuhn et al., 1996). This has been observed through decreased cell proliferation in the SGZ, and a reduced number of RGL stem cells, which also become increasingly quiescent (Kuhn et al., 1996; Encinas et al., 2011; Villeda et al., 2011). A previous study also suggested that the length of the cell cycle in the adult dentate gyrus does not increase with age (Olariu et al., 2007). How the behavior of individual IPCs changes with age in the adult mouse dentate gyrus is not clear. We injected a clonal dose of tamoxifen in 2 and 6 month-old mice and compared the clonal size and differentiation of GFP$^+$ cells at 6 dpi (Figs. 5A and 5B). We observed no change in the size of GFP$^+$ clones (Fig. 5C). Interestingly, we observed an increase in the percentage of neuroblasts and a decrease in the number of immature neurons in the 6 month-old group (Fig. 5D). Together, these results showed that there is no change in the output of individual Tbr2$^+$ IPCs, but their differentiation rate is decreased in older animals.

Discussion

In this study, we describe with unprecedented temporal and cellular resolution that Tbr2$^+$ IPCs are unipotent neuronal progenitor cells and undergo limited clonal expansion prior to differentiating into immature neurons. Additionally, the clone size is not affected by enriched environment or age. Rather, enriched environment accelerates the differentiation process, while aging animals exhibit slower neuronal differentiation.

A large number of granule neurons are added to the dentate gyrus of adult mammals every day (Ernst and Frisén, 2015). For example, it has been estimated that 9000 cells are born daily in the young adult rat hippocampus and 1400 new neurons are added to the human hippocampus (Cameron and McKay, 2001; Spalding et al., 2013). In rodents it has been shown that RGLs are stem cells that fuel neurogenesis, but it

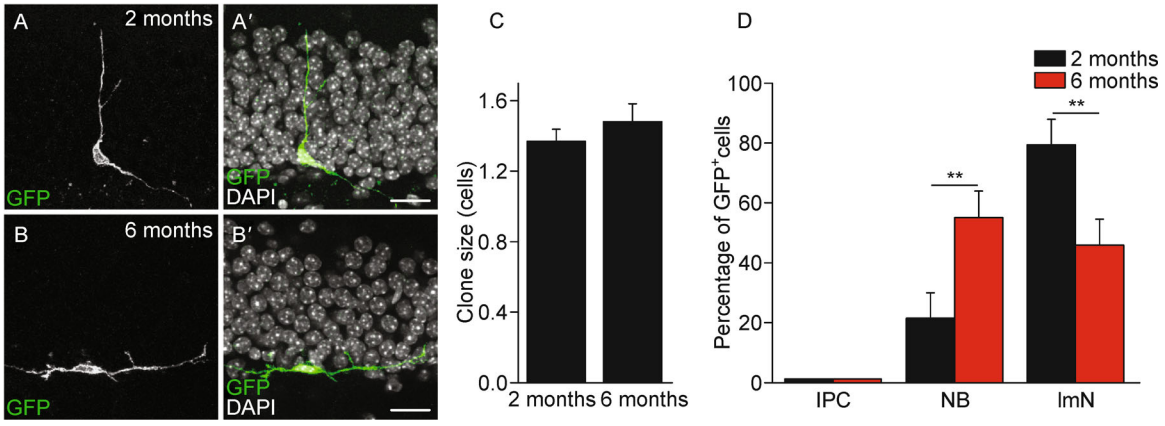

Figure 5 Slower differentiation tempo of Tbr2$^+$ IPCs in the dentate gyrus in older adult mice. (A–B) Sample confocal images of GFP$^+$ immature neurons at 6 dpi from a 2 month-old mouse (A) and GFP$^+$ neuroblasts at 6 dpi from a 6 month-old mouse (B). Scale bars: 20 µm. (C) Quantitative comparison of clonal size at 4 dpi. Values represent mean±SEM (n = 6 dentate gyri). (D) Quantitative comparison of percentages of cell types observed in GFP$^+$ clones at 6 dpi. Values represent mean±SEM (n = 6 dentate gyri; $^{**}p < 0.05$; Student's t-test).

has also been thought that the IPCs act as a transit amplifying population of cells (Encinas et al., 2006). In this study, we did not observe any significant amplification of the *Tbr2*$^+$-*CreER*^{T2}-traced clones. One possibility is that the major amplification step occurs in the Ascl1$^+$ Tbr2$^-$ precursor population, which are not labeled in our *Tbr2-CreER*^{T2} mice. However, a previous study using the *Hes5-CreER* mice has shown that the Ascl1-expressing precursors do not amplify significantly in the adult SGZ (Lugert et al., 2012). Together, these result suggest a model that, unlike IPCs in the adult SVZ, IPCs in the adult SGZ do not undergo a significant amount of amplification, because of either limited rounds of cell division or significant cell death of the progeny, which is known to occur at this stage of development (Sierra et al., 2010; Song et al., 2013).

The transcription factor Tbr2 is expressed in IPCs in both the developing and adult brain (Englund et al., 2005; Hodge et al., 2008). Previous studies using knockout animals have shown that the Tbr2 protein is essential for morphogenesis of the dentate gyrus and the rostral migratory stream from the SVZ (Hodge et al., 2012; Hodge et al., 2013; Kahoud et al., 2014). A *Tbr2-CreER*^{T2} transgenic mouse has previously been used to study embryonic cortical development (Pimeisl et al., 2013; Vasistha et al., 2014). These studies showed that Tbr2$^+$ IPCs give rise to glutamatergic, but not GABAergic neurons or astrocytes. A recent study using clonal analysis showed that individual IPCs in the embryonic cortex, on average give rise to 2 neurons per clone (Gao et al., 2014). These studies, together with the data presented here suggest that IPCs have similar features in development and in the adult brain in terms of cell potential and limited clonal expansion.

We provided clonal lineage tracing evidence that Tbr2$^+$ IPCs are unipotent neuronal precursors under homeostasis in the adult SGZ. EGF infusion into the hippocampus has previously been shown to convert IPCs into multipotent stem cells (Doetsch et al., 2002). Future studies should examine if Tbr2$^+$ cells can dedifferentiate upon EGF infusion or injury, which is also known to alter the behavior of neural precursors in the adult brain (Seri et al., 2001; Jiruska et al., 2013). Different stage of adult neurogenesis can be modulated by the local or external environment. Interestingly, we observed that an enriched environment together with running accelerates the differentiation process of Tbr2$^+$ IPCs. A previous study has shown that running increases network activity in the dentate gyrus and accelerates maturation of immature neurons in the adult dentate gyrus (Piatti et al., 2011). Together with our finding, these results suggests that the running accelerates the development of both IPCs and immature neurons.

We showed that the *Tbr2-CreER*^{T2} mice allow highly specific labeling of a rather homogeneous population of IPCs, which develop into immature neurons in a synchronous manner (Fig. 2). Future studies could make use of the *Tbr2-CreER*^{T2} transgenic mouse line to target and genetically manipulate a cohort of newborn neurons with similar birthdates in the adult dentate gyrus *in vivo*. When combined with genetically encoded activity indicators, *in vivo* electrophysiological recordings and optogenetic tools, this model could be used to decipher properties of newborn neurons at specific developmental stages in behaving animals and how they contribute to specific brain functions.

Acknowledgements

This work was supported by NIH (NS048271 and MH105128 to G-l. M., NS047344 and ES021957 to H.S., NS093772 to H.S. and K.M. C.). D.A.B. was supported by EMBO long-term postdoctoral fellowship and postdoctoral grant from the Swedish Research Council (Vetenskapsrådet). K.Y. was supported by long-term postdoctoral fellowship by Human Frontier Science Program.

Compliance with ethics guidelines

Daniel A. Berg, Ki-Jun Yoon, Brett Will, Alex Y. Xiao, Nam-Shik Kim, Kimberly M. Christian, Hongjun Song and Guo-li Ming declare that they have no conflict of interest. All institutional and national guidelines for the care and use of laboratory animals were followed.

References

Andersen J, Urbán N, Achimastou A, Ito A, Simic M, Ullom K, Martynoga B, Lebel M, Göritz C, Frisén J, Nakafuku M, Guillemot F (2014). A transcriptional mechanism integrating inputs from extracellular signals to activate hippocampal stem cells. Neuron, 83 (5): 1085–1097

Bonaguidi M A, Wheeler M A, Shapiro J S, Stadel R P, Sun G J, Ming G L, Song H (2011). *In vivo* clonal analysis reveals self-renewing and multipotent adult neural stem cell characteristics. Cell, 145(7): 1142–1155

Braun S M G, Jessberger S (2013). Adult neurogenesis in the mammalian brain. Front Biol, 8(3): 295–304

Brown J P, Couillard-Després S, Cooper-Kuhn C M, Winkler J, Aigner L, Kuhn H G (2003). Transient expression of doublecortin during adult neurogenesis. J Comp Neurol, 467(1): 1–10

Calzolari F, Michel J, Baumgart E V, Theis F, Götz M, Ninkovic J (2015). Fast clonal expansion and limited neural stem cell self-renewal in the adult subependymal zone. Nat Neurosci, 18(4): 490–492

Cameron H A, McKay R D (2001). Adult neurogenesis produces a large pool of new granule cells in the dentate gyrus. J Comp Neurol, 435 (4): 406–417

DeCarolis N A, Mechanic M, Petrik D, Carlton A, Ables J L, Malhotra S, Bachoo R, Götz M, Lagace D C, Eisch A J (2013). *In vivo* contribution of nestin- and GLAST-lineage cells to adult hippocampal neurogenesis. Hippocampus, 23(8): 708–719

Doetsch F, Petreanu L, Caille I, Garcia-Verdugo J M, Alvarez-Buylla A (2002). EGF converts transit-amplifying neurogenic precursors in the adult brain into multipotent stem cells. Neuron, 36(6): 1021–1034

Encinas J M, Michurina T V, Peunova N, Park J H, Tordo J, Peterson D A, Fishell G, Koulakov A, Enikolopov G (2011). Division-coupled astrocytic differentiation and age-related depletion of neural stem cells in the adult hippocampus. Cell Stem Cell, 8(5): 566–579

Encinas J M, Vaahtokari A, Enikolopov G (2006). Fluoxetine targets early progenitor cells in the adult brain. Proc Natl Acad Sci USA, 103 (21): 8233–8238

Englund C, Fink A, Lau C, Pham D, Daza R A, Bulfone A, Kowalczyk T, Hevner R F (2005). Pax6, Tbr2, and Tbr1 are expressed sequentially by radial glia, intermediate progenitor cells, and postmitotic neurons in developing neocortex. J Neurosci, 25(1): 247–251

Ernst A, Frisén J (2015). Adult neurogenesis in humans- common and unique traits in mammals. PLoS Biol, 13(1): e1002045

Faulkner R L, Jang M H, Liu X B, Duan X, Sailor K A, Kim J Y, Ge S, Jones E G, Ming G L, Song H, Cheng H J (2008). Development of hippocampal mossy fiber synaptic outputs by new neurons in the adult brain. Proc Natl Acad Sci USA, 105(37): 14157–14162

Gao P, Postiglione M P, Krieger T G, Hernandez L, Wang C, Han Z, Streicher C, Papusheva E, Insolera R, Chugh K, Kodish O, Huang K, Simons B D, Luo L, Hippenmeyer S, Shi S H (2014). Deterministic progenitor behavior and unitary production of neurons in the neocortex. Cell, 159(4): 775–788

Ge S, Goh E L, Sailor K A, Kitabatake Y, Ming G L, Song H (2006). GABA regulates synaptic integration of newly generated neurons in the adult brain. Nature, 439(7076): 589–593

Hodge R D, Garcia A J 3rd, Elsen G E, Nelson B R, Mussar K E, Reiner S L, Ramirez J M, Hevner R F (2013). Tbr2 expression in Cajal-Retzius cells and intermediate neuronal progenitors is required for morphogenesis of the dentate gyrus. J Neurosci, 33(9): 4165–4180

Hodge R D, Kowalczyk T D, Wolf S A, Encinas J M, Rippey C, Enikolopov G, Kempermann G, Hevner R F (2008). Intermediate progenitors in adult hippocampal neurogenesis: Tbr2 expression and coordinate regulation of neuronal output. J Neurosci, 28(14): 3707–3717

Hodge R D, Nelson B R, Kahoud R J, Yang R, Mussar K E, Reiner S L, Hevner R F (2012). Tbr2 is essential for hippocampal lineage progression from neural stem cells to intermediate progenitors and neurons. J Neurosci, 32(18): 6275–6287

Jang M H, Bonaguidi M A, Kitabatake Y, Sun J, Song J, Kang E, Jun H, Zhong C, Su Y, Guo J U, Wang M X, Sailor K A, Kim J Y, Gao Y, Christian K M, Ming G L, Song H (2013). Secreted frizzled-related protein 3 regulates activity-dependent adult hippocampal neurogenesis. Cell Stem Cell, 12(2): 215–223

Jiruska P, Shtaya A B, Bodansky D M, Chang W C, Gray W P, Jefferys J G (2013). Dentate gyrus progenitor cell proliferation after the onset of spontaneous seizures in the tetanus toxin model of temporal lobe epilepsy. Neurobiol Dis, 54: 492–498

Kahoud R J, Elsen G E, Hevner R F, Hodge R D (2014). Conditional ablation of Tbr2 results in abnormal development of the olfactory bulbs and subventricular zone-rostral migratory stream. Dev Dyn, 243(3): 440–450

Kempermann G, Kuhn H G, Gage F H (1997). More hippocampal neurons in adult mice living in an enriched environment. Nature, 386 (6624): 493–495

Kim E J, Ables J L, Dickel L K, Eisch A J, Johnson J E (2011). Ascl1 (Mash1) defines cells with long-term neurogenic potential in subgranular and subventricular zones in adult mouse brain. PLoS ONE, 6(3): e18472

Kim J Y, Liu C Y, Zhang F, Duan X, Wen Z, Song J, Feighery E, Lu B, Rujescu D, St Clair D, Christian K, Callicott J H, Weinberger D R, Song H, Ming G L (2012). Interplay between DISC1 and GABA signaling regulates neurogenesis in mice and risk for schizophrenia. Cell, 148(5): 1051–1064

Kronenberg G, Reuter K, Steiner B, Brandt M D, Jessberger S, Yamaguchi M, Kempermann G (2003). Subpopulations of proliferating cells of the adult hippocampus respond differently to physiological neurogenic stimuli. J Comp Neurol, 467(4): 455–463

Kuhn H G, Dickinson-Anson H, Gage F H (1996). Neurogenesis in the dentate gyrus of the adult rat: age-related decrease of neuronal progenitor proliferation. J Neurosci, 16(6): 2027–2033

Liu P, Jenkins N A, Copeland N G (2003). A highly efficient recombineering-based method for generating conditional knockout mutations. Genome Res, 13(3): 476–484

Lugert S, Basak O, Knuckles P, Haussler U, Fabel K, Götz M, Haas C A, Kempermann G, Taylor V, Giachino C (2010). Quiescent and active hippocampal neural stem cells with distinct morphologies respond selectively to physiological and pathological stimuli and aging. Cell Stem Cell, 6(5): 445–456

Lugert S, Vogt M, Tchorz J S, Müller M, Giachino C, Taylor V (2012). Homeostatic neurogenesis in the adult hippocampus does not involve amplification of Ascl1(high) intermediate progenitors. Nat Commun, 3: 670

Ming G L, Song H (2011). Adult neurogenesis in the mammalian brain: significant answers and significant questions. Neuron, 70(4): 687–702

Muzumdar M D, Tasic B, Miyamichi K, Li L, Luo L (2007). A global double-fluorescent Cre reporter mouse. Genesis, 45(9): 593–605

Olariu A, Cleaver K M, Cameron H A (2007). Decreased neurogenesis in aged rats results from loss of granule cell precursors without lengthening of the cell cycle. J Comp Neurol, 501(4): 659–667

Piatti V C, Davies-Sala M G, Espósito M S, Mongiat L A, Trinchero M F, Schinder A F (2011). The timing for neuronal maturation in the adult hippocampus is modulated by local network activity. J Neurosci, 31(21): 7715–7728

Pimeisl I M, Tanriver Y, Daza R A, Vauti F, Hevner R F, Arnold H H, Arnold S J (2013). Generation and characterization of a tamoxifen-inducible Eomes (CreER) mouse line. Genesis, 51(10): 725–733

Ponti G, Obernier K, Guinto C, Jose L, Bonfanti L, Alvarez-Buylla A (2013). Cell cycle and lineage progression of neural progenitors in the ventricular-subventricular zones of adult mice. Proc Natl Acad Sci USA, 110(11): E1045–E1054

Seri B, García-Verdugo J M, McEwen B S, Alvarez-Buylla A (2001). Astrocytes give rise to new neurons in the adult mammalian hippocampus. J Neurosci, 21(18): 7153–7160

Sessa A, Mao C A, Hadjantonakis A K, Klein W H, Broccoli V (2008). Tbr2 directs conversion of radial glia into basal precursors and guides neuronal amplification by indirect neurogenesis in the developing neocortex. Neuron, 60(1): 56–69

Sierra A, Encinas J M, Deudero J J, Chancey J H, Enikolopov G, Overstreet-Wadiche L S, Tsirka S E, Maletic-Savatic M (2010). Microglia shape adult hippocampal neurogenesis through apoptosis-coupled phagocytosis. Cell Stem Cell, 7(4): 483–495

Song J, Sun J, Moss J, Wen Z, Sun G J, Hsu D, Zhong C, Davoudi H, Christian K M, Toni N, Ming G L, Song H (2013). Parvalbumin interneurons mediate neuronal circuitry-neurogenesis coupling in the adult hippocampus. Nat Neurosci, 16(12): 1728–1730

Song J, Zhong C, Bonaguidi M A, Sun G J, Hsu D, Gu Y, Meletis K, Huang Z J, Ge S, Enikolopov G, Deisseroth K, Luscher B, Christian K M, Ming G L, Song H (2012). Neuronal circuitry mechanism regulating adult quiescent neural stem-cell fate decision. Nature, 489 (7414): 150–154

Spalding K L, Bergmann O, Alkass K, Bernard S, Salehpour M, Huttner H B, Boström E, Westerlund I, Vial C, Buchholz B A, Possnert G, Mash D C, Druid H, Frisén J (2013). Dynamics of hippocampal neurogenesis in adult humans. Cell, 153(6): 1219–1227

Srinivas S, Watanabe T, Lin C S, William C M, Tanabe Y, Jessell T M, Costantini F (2001). Cre reporter strains produced by targeted insertion of EYFP and ECFP into the ROSA26 locus. BMC Dev Biol, 1(1): 4

Steiner B, Zurborg S, Hörster H, Fabel K, Kempermann G (2008). Differential 24 h responsiveness of Prox1-expressing precursor cells in adult hippocampal neurogenesis to physical activity, environmental enrichment, and kainic acid-induced seizures. Neuroscience, 154(2): 521–529

Sun G J, Sailor K A, Mahmood Q A, Chavali N, Christian K M, Song H, Ming G L (2013). Seamless reconstruction of intact adult-born neurons by serial end-block imaging reveals complex axonal guidance and development in the adult hippocampus. J Neurosci, 33(28): 11400–11411

Toni N, Laplagne D A, Zhao C, Lombardi G, Ribak C E, Gage F H, Schinder A F (2008). Neurons born in the adult dentate gyrus form functional synapses with target cells. Nat Neurosci, 11(8): 901–907

van Praag H, Kempermann G, Gage F H (1999). Running increases cell proliferation and neurogenesis in the adult mouse dentate gyrus. Nat Neurosci, 2(3): 266–270

van Praag H, Schinder A F, Christie B R, Toni N, Palmer T D, Gage F H (2002). Functional neurogenesis in the adult hippocampus. Nature, 415(6875): 1030–1034

Vasistha N A, Garcia-Moreno F, Arora S, Cheung A F, Arnold S J, Robertson E J, Molnar Z (2014). Cortical and clonal contribution of Tbr2 expressing progenitors in the developing mouse brain. Cereb Cortex, pii: bhu125. [Epub ahead of print]

Villeda S A, Luo J, Mosher K I, Zou B, Britschgi M, Bieri G, Stan T M, Fainberg N, Ding Z, Eggel A, Lucin K M, Czirr E, Park J S, Couillard-Després S, Aigner L, Li G, Peskind E R, Kaye J A, Quinn J F, Galasko D R, Xie X S, Rando T A, Wyss-Coray T (2011). The ageing systemic milieu negatively regulates neurogenesis and cognitive function. Nature, 477(7362): 90–94